RSC Advances

ROYAL SOCIETY OF CHEMISTRY

www.rsc.org/advances

RSC Advance

RSCPublishing

ARTICLE

Efficient Robust Fluorite $CeZrO_{4-\delta}$ oxide Catalyst for the Eco-benign Synthesis of Styrene

Cite this: DOI: 10.1039/x0xx00000x

Kaliyappan Periyasamy[a], Aswathy T Venugopalan [a], Venugopal Ashok kumar[a], Marimuthu Manikandan[a], Rakesh Shukla[b], Avesh K Tyagi[b*] and Thirumalaiswamy Raja[a*]

Received 00th January 2012,
Accepted 00th January 2012

DOI: 10.1039/x0xx00000x

www.rsc.org/

In this work, we have reported CeO_2, ZrO_2, physically mixed (PH)-CeO_2/ZrO_2 and fluorite $CeZrO_{4-\delta}$ oxides and their catalytic activities for the oxidative dehydrogenation (ODH) of ethyl benzene (EB) to styrene (ST) using molecular oxygen, air and carbon dioxide as oxidants. Catalysts were prepared by gel-combustion method followed by calcination at 600˚C for 6 h and subjected to catalytic activity measurements. All the catalysts were characterized and studied by various physicochemical methods. Reaction parameters were varied systematically such as different catalysts, oxidants, temperatures, EB flow and oxidant flow. $CeZrO_{4-\delta}$ accounted for 47% styrene yield for 72 hr without any significant deactivation under optimized reaction conditions. A thorough analysis of spent catalysts demonstrated the robustness of the catalyst for this reaction under different oxidants and reaction conditions. Pristine CeO_2 deactivated easily and the activity decreased as time on stream of the reaction.

Introduction:

Ethyl benzene (EB) to styrene (ST) is a commercially important pathway in polymer and petrochemical industries. Styrene is an important monomer for the production of polystyrene, plastics, styrence-acrylonitrile, styrene butadiene latex and other copolymers.[1]Commercially styrene is produced by dehydrogenation of ethyl benzene using potassium promoted hematite catalysts with superheated steam at 700˚C.[2] This dehydrogenation reaction is a highly endothermic process and the stringent reaction conditions are the main drawback. To overcome this, oxidative dehydrogenation (ODH) of EB is an alternative process for the production of ST to realize an exothermic reaction and shift entirely the equilibrium towards the desired product formation and to carry out the reaction at lower temperature. ODH of EB to ST is one of the most industrially important reactions which possess the challenge of tailoring of suitable catalysts and relatively non stringent reaction conditions. Use of soft oxidants like CO_2[3-4], N_2O[5-6], O_2[7] and air[8-9] are environmentally benign process. Venugopal *et al* had reported that the ceria supported hydrotalcite catalyst has maximum conversion for ethyl benzene using oxygen as an oxidant.[7] They also reported that ceria loading is directly proportional to the conversion and selectivity.[7] Reddy *et al* carried out oxidative dehydrogenation of EB using air over $V_2O_5/Ce_xZr_{1-x}O_2/SiO_2$ catalysts[8] and also they investigated the EB to ST conversion using air as oxidant on CeO_2/Al_2O_3 and $V_2O_5/CeO_2/Al_2O_3$ as catalysts.[10] Xiao *et al* have reported the ODH of EB using hierarchical porous carbon spheres using molecular oxygen giving around 43% conversion.[11] Takehira and co-workers were reported oxidative dehydrogenation of EB using CO_2 and O_2 over Mg-Fe-Al mixed oxide derived hydrotalcite catalyst.[12] Vansant *et al* had reported dehydrogenation of EB using N_2O over transition metals supported on mesoporous silica materials. They found Fe^{3+} is active for EB conversion.[6]

Ceria is well known for its redox properties[13] and oxygen storage capacity, which is used in many catalytic reactions and three way catalyst.[14,15] Fan *et al.* have reported mesostructured ceria which shows 34% conversion and 87% selectivity in EB conversion.[16] Pure ceria shows low catalytic activity at higher temperatures because of its poor thermal stability.[10,17] To overcome these disadvantages, ceria is incorporated in oxides and component of mixed oxide catalysts which shows improved activity and thermal stability.[9] Ceria-based mixed oxide catalysts are widely used in many organic reactions[18] and also in selective oxidation reactions.[19] Zirconia has good oxygen storage capacity and thermal stability. In many reactions, ceria-zirconia catalyst shows better catalytic activity, thermal stability and oxygen storage/evolution capacity. When zirconia is incorporated in ceria lattice it enhances the oxygen storage capacity [20] and thermal stability.[20,21] Di Monte *et al* reported that ceria-zirconia mixed oxide shows high redox property and thermal stability in heterogeneous catalysis.[22]

Herein, we reported the use of a $CeZrO_{4-\delta}$ as catalyst for the industrially important oxidative dehydrogenation of EB to ST. We have prepared $CeZrO_{4-\delta}$ with fluorite structure, CeO_2 and ZrO_2 by gel-combustion method, while PH-CeO_2/ZrO_2 was prepared by physical mixture method. These catalysts were subjected to characteristic techniques such as XRD, HRTEM, Raman analysis, APPES, TGA and N_2 adsorption. It was subjected to the catalytic activity of oxidative dehydrogenation of ethyl benzene to styrene. The catalytic stability was tested for long time on stream (TOS) of 72h.

EXPERIMENTAL SECTION:

CATALYST PREPARATION:

To get better powder properties for catalysis, instead of the stoichiometric oxidant-to-fuel ratio reported for the method, a fuel-deficient ratio was selected in this case. All catalysts were prepared by gel-combustion method. Cerium (III) Nitrate (Alfa Aesar), Zirconyl (IV) Nitrate (Loba Chemie) as oxidant and Glycine as fuel (Merck) were used as precursor for catalyst synthesis. Calculated amount of standard solution of zirconyl nitrate and cerium nitrate were dissolved in distilled water. To this solution, glycine (60% fuel deficient ratio i.e for 1 mmol of cerium nitrate and zirconyl nitrate each, 2 mmol of glycine) was added followed by evaporation near to dryness on a hot plate to form a transparent colorless gel. On further heating on the hot plate, the gel undergoes auto-ignition to form a fluffy mass. The obtained powder was calcined at 600˚C for 6 hours. We used cerium nitrate as a precursor for pure ceria and zirconyl nitrate as a precursor for pure zirconia catalyst. Preparation method of pure ceria and pure zirconia was as same as above procedure. Above mentioned catalysts were labeled as $CeZrO_{4-\delta}$, CeO_2 and ZrO_2. Physically mixed CeO_2/ZrO_2catalyst was prepared by simply mixing cerium nitrate and zirconyl nitrate together and milled with proper ratio. The obtained powder was calcined at 600˚C for 6 hours and the catalyst was labelled as PH-CeO_2/ZrO_2.

The as-synthesized and spent materials were characterized by Powder X-ray diffraction (PXRD) and the data were collected on PANalytical X'pert Pro dual goniometer diffractometer using Cu- Kα (1.5418Å) radiation with Ni filter with a step size of 0.008°and a scan rate of 0.5° min^{-1}. Crystallite size of the catalysts was calculated by using scherrer's formulae. Nitrogen adsorption/desorption isotherms were collected from Quantachrome USA. The samples were degassed at 250˚C for 3 h under vacuum to remove moisture and other volatiles. Surface area was calculated by Brunauer–Emmett–Teller (BET) equation from the adsorption branch. EDX measurements were done on an SEM system (FEI, Model Quanta 200 3D) equipped with EDX facility. EDX spectra were recorded in the spot-profile mode by focusing the electron beam onto specific regions of the sample. High resolution transmission electron microscopies (HR-TEM) of all materials were recorded using FEI TECNAI F30 electron microscope operating at 300 kV. Samples were powdered and dispersed in isopropanol before depositing onto a holey carbon grid. Perkin Elmer Diamond's thermogravimetry (TG) instrument was used to measure the thermal analysis of spent catalyst. Raman spectra were recorded on a Horiba JY LabRAMHR800 Raman spectrometer coupled with microscope in reflectance mode with 514 nm excitation laser source. XPS measurement for the $CeZrO_{4-\delta}$ catalyst was done by ambient pressure photoelectron spectrometer (APPES) under UHV condition. X-rays are generated by Mg Kα X-ray source for XPS measurement.

CATALYTIC ACTIVITY:

The catalytic evaluation study was performed by using a fixed bed continuous up flow reactor (FBR) having two furnace zones under atmospheric pressure. In the typical experiment, catalytic bed was placed at centre of the reactor loaded with 1.0mL of catalyst (0.9g catalyst), above and below of the catalytic bed was filled with ceramic beads. A reactor tube (inconel) with 13 mm internal diameter and 510 mm length was used to pack the catalyst. The catalyst was pelletized and sieved through the mesh size of 0.5-0.8mm. The temperature of the reactor and in the catalyst bed was measured using a K-type coaxially centered thermocouple. EB feed flow of liquid hourly space velocity (LHSV) 3 h^{-1} was controlled by isocratic pump (Lab Alliance Series II) and the optimized oxygen, carbon dioxide and air flow with gas hourly space velocity (GHSV) 2400 h^{-1} was controlled by using a Brooks's make mass flow controller (5890E series). The mole ratio of O_2/EB is 4. The feed flow was configured to operate up flow mode and the products were condensed using a chiller. The liquid products were analyzed using varian CP 3800 gas chromatography with HP-5 column (30m x 0.32m x 0.25m) along with FID detector. The gas analysis was done by TCD detector with Molecular Sieve 5A. Conversion and selectivity of the ethyl benzene and styrene was calculated as per procedures described elsewhere.[9]

RESULTS AND DISCUSSION:

POWDER X-RAY DIFFRACTION:

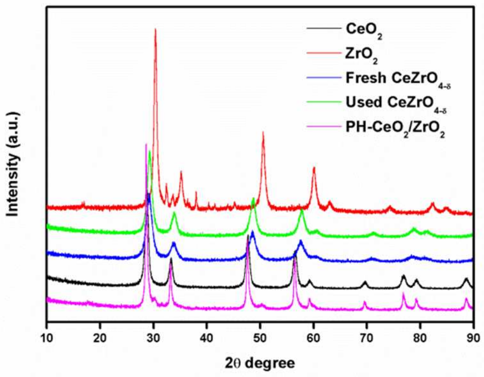

Fig. 1. Powder X-ray diffraction pattern of CeO_2, ZrO_2, PH-CeO_2/ZrO_2, fresh and used $CeZrO_{4-\delta}$ catalysts.

Powder X-Ray Diffraction pattern for as-synthesized CeO_2, ZrO_2, PH-CeO_2/ZrO_2, fresh and spent $CeZrO_{4-\delta}$ catalysts are shown in Fig.7. Powder X-ray diffraction pattern of $CeZrO_{4-\delta}$ catalyst calcined at 600˚C shows seven major peaks (111), (200), (220), (311), (222), (400) and (331) at 29.1˚, 33.6˚, 48.5˚, 57.6˚, 60.2˚, 71.2˚, 78.5˚ respectively which corresponds to cubic fluorite structure (JCPDS 38-1439). The weak cation ordered peaks for pyrochlore related $Ce_2Zr_2O_8$ could not be observed in the XRD.[23] The absence of cation ordering may be explained as follows. The fuel-deficient ratio was selected for the gel-combustion reaction, the exothermicity in the reaction was low and the heat generated was not sufficient enough for the formation of cation ordered form of this compound. Probably this could be the main reason to obtain $CeZrO_{4-\delta}$ instead of cation ordered $Ce_2Zr_2O_8$. From the most intense (111) peak at 2θ=29.1˚ is used to take FWHM value and the crystallite size was calculated. The crystallite size for $CeZrO_{4-\delta}$ catalyst is ~ 6 nm. Surface area and crystallite size of as prepared catalyst are given in **Table.1.**

Table.1. Surface area and crystallite size of as-prepared catalyst

S.No.	Sample	Crystallite Size (nm)^a	Surface Area (m^2/g)	Pore Volume (cc/g)^b
1.	$CeZrO_{4-\delta}$	6.2	31	0.18
2	CeO_2	11.0	37	0.16
3	ZrO_2	13.5	23	0.14
4	PH-CeO_2/ZrO_2	28.8	22	0.16

^{a}Average crystallite size calculated from Scherrer equation ^{b}Pore Volume from BET surface area.

Surface area depends on crystallite size, when the size of the particles decreases surface area increases and vice versa. Surface area of pure ceria was 37m^2/g, which is higher compare to other catalysts. When zirconia is incorporated into the ceria lattice, surface area is decreased to 31m^2/g which may be due to insertion of zirconia into ceria and increase in crystallinity and leads to decrease in the specific surface area.[24] Pure zirconia and physical mixture of CeO_2/ZrO_2 shows low surface area compared to other catalysts.

RAMAN SPECTROSCOPY:

Raman spectra for as-prepared ceria catalyst shows only one high intensity peak at 465 cm^{-1} corresponds to typical Raman active cubic fluorite F2g CeO_2. For zirconia, Raman spectrum shows six peaks corresponds to tetragonal phase of ZrO_2.[25] Typical Raman spectrum of CeO_2, ZrO_2, fresh and used $CeZrO_{4-\delta}$ catalysts are shown in Fig.2. Raman spectra of $CeZrO_{4-\delta}$ catalyst shows a high intense peak at 473 cm^{-1} and two broad shoulder peaks at 310 and 620 cm^{-1}. There is no tetragonal phase for zirconia in $CeZrO_{4-\delta}$ catalyst which means that the ceria and zirconia form a solid solution and stabilize in the single phase fluorite structure. The absence of the Raman shift of the pyrochlore modes also confirms the stabilization of fluorite phase, which is in accordance with XRD data. The strong intense peak at 473 cm^{-1} (inset) corresponds to ceria. The progressive shift of ceria peak from 465 to 473 cm^{-1} is due to the cell contraction attributed to zirconia incorporation in the ceria lattice.[26] The incorporation of zirconia into ceria is further confirmed as there is decrease of lattice parameter of the product compared to that of parent ceria. A shift is observed in the broad F2g peak to 473 cm^{-1}. This blue shift indicated the change in chemical interaction and lattice parameters possibly due to the incorporation of Zr in ceria lattice.[27,28] The peak at 310 cm^{-1} shows presence of change in the position of the oxygen atom from their ideal fluorite structure. The broad and weak peak at 620 cm^{-1} attributes to Raman inactive of lattice oxygen mode in $CeZrO_{4-\delta}$ catalyst. The appearance of this peak is due to presence of oxygen vacancy in the fluorite phase which causes defects sites in Ce-Zr oxides for the activity of the catalyst. Full width at half maximum (FWHM) of F2g peak of ceria in the mixed oxide can be used to measure the oxygen vacancies in the catalyst. An increasing amount of Zr incorporation in CeO_2 lattice along with increasing oxygen vacancies are possible reason for the above changes in Raman spectra.

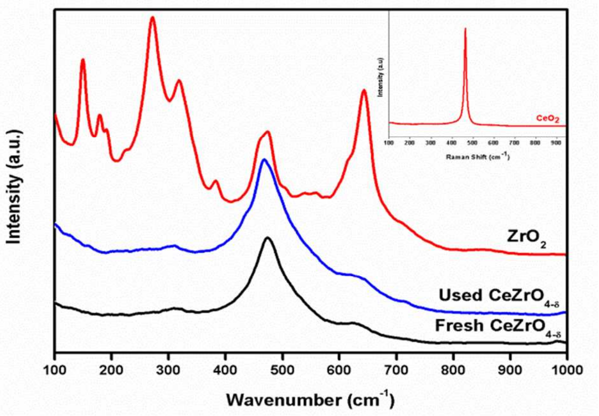

Fig.2. Raman spectroscopy of the CeO_2, ZrO_2, Fresh and used $CeZrO_{4-\delta}$ catalysts.

TRANSMISSION ELECTRON MICROSCOPY (TEM):

Morphology and textural properties of the $CeZrO_{4-\delta}$ catalyst has been studied by HR-TEM. Average size of the crystallites was apparently reduced, and what cause this size reduction is unknown HRTEM images of the $CeZrO_{4-\delta}$ catalyst at low resolution (**Fig.3a and 3b**) and high resolution (**Fig.3c and 3d**) were shown in **Fig.3.** The particle size was measured for $CeZrO_{4-\delta}$ catalyst; it shows 6±1 nm which is good agreement with XRD data. Selected Area Electron Diffraction (SAED) confirmed the crystalline nature of the $CeZrO_{4-\delta}$ catalyst which is shown in inset image in **Fig.3d (i)**. The d-spacing value of ~3.1Å and ~2.8Å shows the (111) and (200) planes respectively for $CeZrO_{4-\delta}$ catalyst. These d-spacing values further confirm the fluorite nature of the $CeZrO_{4-\delta}$ sample.

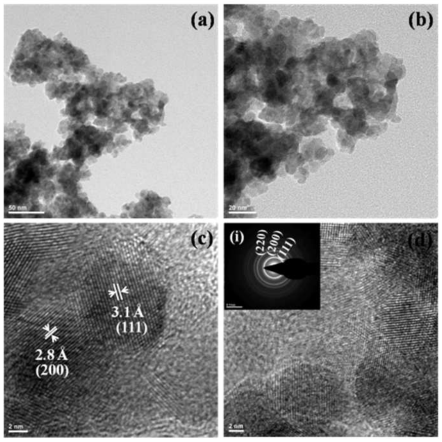

Fig.3. TEM images of the $CeZrO_{4-\delta}$ fresh catalyst Calcined at 600°C. (a), (b) low resolution and (c), (d) high resolution (inset: SAED pattern).

A disordered mesoporous structure was observed for $CeZrO_{4-\delta}$ catalyst. HRTEM image shows the majority of lattice fringes corresponding to ceria-zirconia (111) (d = 0.31 nm) facets of cubic fluorite structure. These observations are in excellent agreement with XRD results. Disordered mesoporous nature has further advantages like low diffusional barriers, since the depth of mesopores are minimum to a few nanometres, unlike several hundred nanometres in conventional ordered mesoporous materials, like MCM-41 and SBA-15.[29] This type of interface is crucial for the transport of reactants, especially oxygen, across the interface from ceria to zirconia, possibly through reverse spill-over phenomenon.

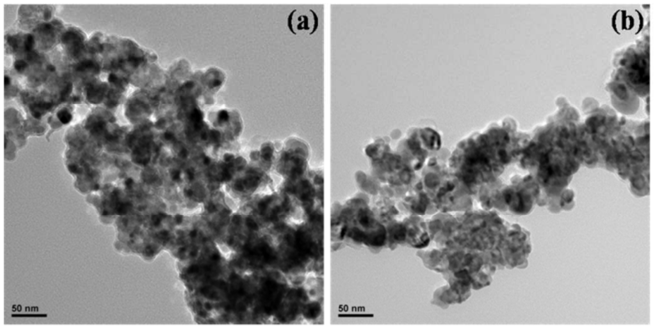

Fig.4. TEM images of the used $CeZrO_{4-\delta}$ catalyst (a) and (b) (Optimized reaction conditions at 72hrs)

To confirm the stability of $CeZrO_{4-\delta}$ catalyst, HRTEM studies for used catalyst (72 hours time on stream). HRTEM images of used $CeZrO_{4-\delta}$ catalyst (72 hours) are shown in **Fig. 4a and 4b**. It clearly shows that there is no change in morphology of the catalyst after 72 hours reaction at optimized reaction conditions. Some amount of carbon is deposited on the surface of the catalyst is clearly observed in HRTEM image. TGA confirms that the carbon deposited on the catalyst around 3.1%.

X-RAY PHOTOELECTRON SPECTROSCOPY (XPS):

To understand the surface of the catalyst and oxidation state of $CeZrO_{4-\delta}$ catalyst, the catalyst was subjected to x-ray photoelectron spectroscopy (XPS). Ceria has two oxidation states such as +3 and +4 oxidation states; it switches over the oxidation state, which causes redox property of the ceria. Fig.5. shows the XPS spectra of Ce 3d. In the XPS spectra of $CeZrO_{4-\delta}$ catalyst, ceria shows the presence of both Ce^{4+} and Ce^{3+} peaks. In Ce 3d XPS spectra, Ce^{4+} shows Ce $3d_{5/2}$ and Ce $3d_{3/2}$ peaks, the binding energy of Ce^{4+} $3d_{3/2}$ are 900.8 eV(u), 907.2 eV(u''), 916.7 eV(u''') respectively and the peaks at 882.4 eV(v), 888.8 eV(v''), 898.1 eV(v''') are corresponding to the binding energy of Ce^{4+} $3d_{5/2}$ respectively.[30-31] For Ce^{3+}, it has four peaks at 903.7 eV(u'), 884.7 eV(v'), 899.2 eV(u_0), and 880.1 eV(v_0) respectively.[30-32] In Ce 3d spectra of $CeZrO_{4-\delta}$ catalyst shows similar binding energy for all peaks compared with pure ceria. But the intensity of Ce^{3+} was higher than pure ceria, which shows more defects sites in $CeZrO_{4-\delta}$ catalysts. Ce^{3+} and Ce^{4+} oxidation state of $CeZrO_{4-\delta}$ catalyst were confirmed by the Ce 3d spectra. Incorporation of zirconia into ceria increases the redox property of ceria and more defect sites generated, which favoured for ODH of EB to ST.

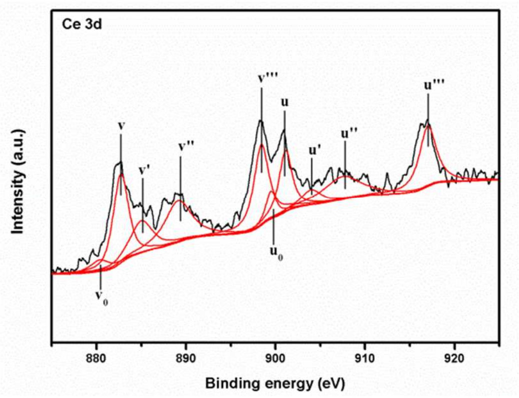

Fig.5. Ce 3d spectra of $CeZrO_{4-\delta}$ catalyst

XPS spectrum of Zr 3d and O 1s are shown in **Fig. 6.** In pure ceria, the binding energy of oxygen 1s spectra peaks at 528.6, 528.8, 529.6 and 530.1 eV were observed which are in agreement with reported values of literature.[29,33] For zirconia, the binding energy of oxygen 1s spectra peak at 530.6 eV which is also in agreement with literature.[34] In the $CeZrO_{4-\delta}$ catalyst, only two O 1s peaks were observed at 529.7 and 531.1 eV which corresponds to lattice oxygen and surface hydroxyl group respectively.[7,35] Fig.11.(b) shows zirconium 3d spectra which clearly shows most prominent peak at 181.1 eV corresponding to Zr $3d_{5/2}$ and low intense peak at 184.2 eV corresponding to Zr$3d_{3/2}$ peak, it indicates that zirconia is in Zr^{4+} oxidation state.[36]

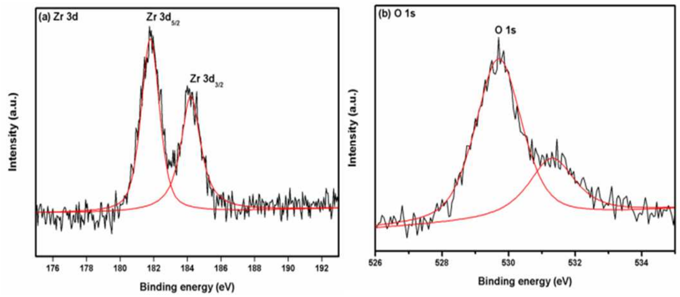

Fig.6. XPS spectrum of $CeZrO_{4-\delta}$ catalyst (a) Zr 3d and (b) O 1s.

CATALYTIC ACTIVITY:

EFFECT OF TEMPERATURE:

Temperature is an important governing parameter for EB to ST conversion. Although EB conversion is directly proportional to increase in reaction temperature, but above an optimum temperature, combustion is always favoured and unavoidable; this leads to decrease in the overall ST yield. To optimize reaction temperature for ST yield, studies were carried out in different temperature range between 450°C and 600°C. At distinct temperatures, the catalytic activity of $CeZrO_{4-\delta}$ catalyst differs, with fixed flow of EB and oxygen. Fig.7. shows the temperature profile of ODH of EB. Maximum yield of ST is observed at 550°C with stable catalytic activity. Over 550°C the combustion was mostly favoured. Increase in temperature increased the conversion of EB in certain extent but the selectivity rapidly decreases from 91% to 76%. Decrease in selectivity was observed above 550°C, this may be due to the formation of undesired by-products like CO_x, water and other products. Maximum conversion of 40% and selectivity of 93% was observed at 550°C with stable catalytic activity. Hence, 550°C was taken as the optimum temperature for obtaining a maximum yield of styrene.

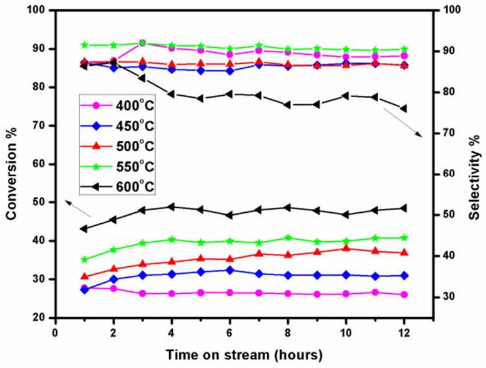

Fig.7. EB conversion and styrene selectivity of the $CeZrO_{4-\delta}$ catalyst on oxidative dehydrogenation of EB at different temperatures (Reaction conditions: 400°C-600°C, LHSV 3 h^{-1} with respect to EB, GHSV 1200 h^{-1} with respect to oxygen, 1 atmosphere pressure, 1mL catalyst)

INFLUENCE OF CONTACT TIME:

To exploit the effect of contact time between reactant and catalytic active site, reaction was carried at with different EB flow at fixed oxygen flow at optimized temperature. EB conversion and ST selectivity of the $CeZrO_{4-\delta}$ catalyst at different reactant flow is shown in Fig.8. We did three different EB flows of LHSV 2, 3 and 5 h^{-1} at 550˚C. While increasing EB flow, there is a constant increase in the conversion of EB but decrease in ST selectivity. We have also observed that lower EB flow (LHSV 2 h^{-1}), has 37% conversion of EB and at LHSV 3 h^{-1} the conversion increased up to 50%. Further increase in EB flow (LHSV 5 h^{-1}), both the conversion and selectivity decreased, which might be due to shorter resident time of reactants over the catalytic active sites. Maximum EB conversion of 50% and ST selectivity of 93% is observed with EB flow LHSV 3 h^{-1} with the function of time. LHSV 3 h^{-1} was taken as the optimum flow for EB based on the above mentioned trend.

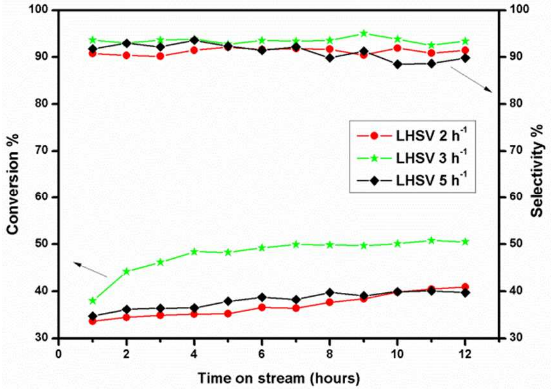

Fig.8. EB conversion and styrene selectivity of the $CeZrO_{4-\delta}$ catalyst on oxidative dehydrogenation of EB at various contact time (Reaction Conditions: 550˚C, GHSV 2400 h^{-1} with respect to oxygen, LHSV 3-5 h^{-1} with respect to EB, 1 atmosphere pressure, 1mL catalyst)

EFFECT OF OXIDANT FLOW:

Catalytic activity of the ODH is also influenced by the oxidant flow. To understand the impact of oxidant flow (O_2) on catalytic activity, we carried out with different flow rate of oxygen (GHSV 600 h^{-1}, 1200 h^{-1} and 2400 h^{-1}). Fig.9 shows effect of oxygen flow in the ODH of EB with different oxidant flow rates, at optimized LHSV 3 h^{-1} with respect to EB flow at 550˚C. Ceria-zirconia catalyst has good oxygen storage capacity and high thermal stability and we are reporting this class of pyrochlore related catalyst for the first time in ODH and it shows the best activity than other catalysts. In this ODH reaction, formation of thin layer of coke in initial hours plays important role in increasing the catalytic activity.[37,7] We observed the maximum conversion of EB and selectivity of styrene is 50% and 93% respectively at GHSV 2400 h^{-1}. Conversion of EB and selectivity towards styrene is increased with increase in oxidant flow rate up to GHSV 2400 h^{-1}. Further increase in oxidant flow (GHSV 3600 h^{-1}), conversion of EB and selectivity towards styrene is decreased rapidly; it may be due to over oxidation which leads to CO_x, water and other unwanted side products. Minimum conversion of EB and selectivity towards styrene is observed in lower oxidant flow of GHSV 600 h^{-1} it may be due to inadequate oxidant. GHSV 2400 h^{-1} with respect to oxidant flow was considered as the optimum flow to achieve maximum yield of styrene.

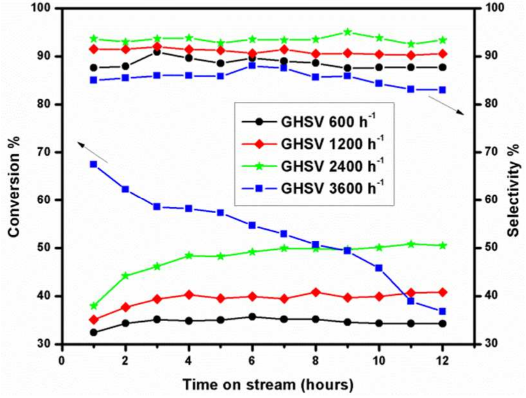

Fig.9. EB conversion and styrene selectivity of the $CeZrO_{4-\delta}$ catalyst on oxidative dehydrogenation of EB at various oxidant flows (Reaction Condition: 550˚C, LHSV 3 h^{-1} with respect to EB, GHSV 600-3600 h^{-1} with respect to oxygen, 1 atmosphere pressure, 1mL catalyst)

In order to study the stability of the catalyst with constant yield of ST by longer time (72hrs) on stream (TOS) reaction was performed under optimized reactions conditions i.e. 550˚C, LHSV 3 h^{-1} with respect to EB and GHSV 2400 h^{-1} with respect to oxygen at atmospheric pressure. The activity of the catalyst remains same for longer duration as in optimized conditions. It is observed from this study that the stability of the catalyst remains stable with only very small decrease in conversion even after 72 hrs. Fig.10. shows the time on stream of $CeZrO_{4-\delta}$ catalyst at optimized reaction condition for EB to ST. Due to it's better oxygen storage/release capacity, poor sinterability and fluorite $CeZrO_{4-\delta}$ phase, it showed constant catalytic activity even after 72 hrs. There is also no change in phase of the catalyst which is confirmed by XRD pattern as shown in Fig.1

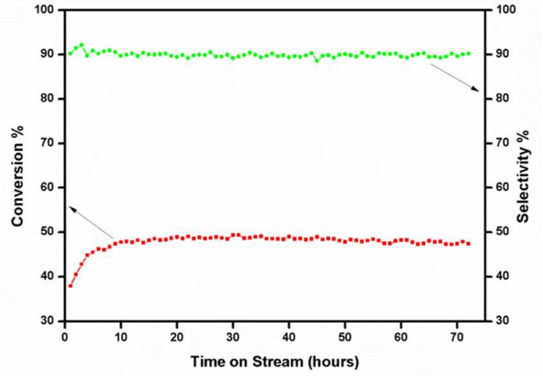

Fig.10. Time on stream study of oxidative dehydrogenation of EB to ST over $CeZrO_{4-\delta}$ catalyst (Reaction Conditions: 550˚C, LHSV 3 h^{-1} with respect to EB, GHSV 2400 h^{-1} with respect to oxygen and 1 atmosphere pressure, 1mL catalyst)

IMPACT OF DIFFERENT PHASES:

Fig.11. shows the catalytic activity of CeO_2, ZrO_2, PH-CeO_2/ZrO_2 and $CeZrO_{4-\delta}$ catalyst under optimized reaction conditions on 18 hours time on stream. To know which phase is active for ODH of EB, these CeO_2, ZrO_2, PH-CeO_2/ZrO_2 and $CeZrO_{4-\delta}$ catalysts were subjected to ODH of EB reaction. CeO_2, ZrO_2 and PH- CeO_2/ZrO_2 catalysts show cubic, tetragonal, cubic/tetragonal phases, respectively. $CeZrO_{4-\delta}$, adopts a fluorite structure as confirmed by XRD data. Pure

ceria shows better conversion at initial time and then rapidly decreased which is usually obtained for ceria. For pure zirconia, the conversion and selectivity was low compared to other catalysts which may be due to coke formation on the catalyst. Compared to $CeZrO_{4-\delta}$ catalyst, $PH-CeO_2/ZrO_2$ catalyst shows low conversion and selectivity towards styrene.

The $CeZrO_{4-\delta}$ catalyst shows maximum conversion and selectivity of 50% and 93% on 18 hours time on stream compared to other catalysts studied. Zirconia shows lowest conversion and selectivity compared to other catalysts.

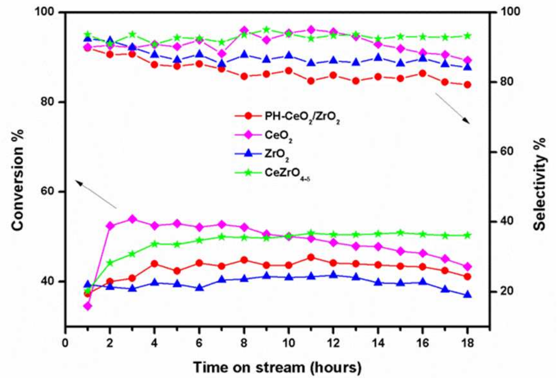

Fig.11. EB conversion and styrene selectivity of the different catalyst on oxidative dehydrogenation of EB (Reaction Condition: 550˚C, LHSV 3 h^{-1} with respect to EB, GHSV 2400 h^{-1} with respect to oxygen, 1 atmosphere pressure, 1mL catalyst)

In $CeZrO_{4-\delta}$ catalyst, selectivity towards styrene is highest (93%) among other catalyst. For pure ceria, zirconia and physical mixture of ceria-zirconia shows low selectivity towards styrene because of formation of by-products like benzene, toluene, styrene oxide and CO_x. Conversion and selectivity of different catalysts is shown in **Table.2.**

Table.2. Conversion and Selectivity of the different catalysts on ODH of EB

Catalyst	Conversion % (EB)	Selectivity %					Yield % (ST)
		ST[d]	BZ[e]	TU[f]	SO[g]	CO_x	
CeO_2	43	86	1.5	4.2	--	8.3	36
ZrO_2	37	84	--	2.4	1.4	12.2	31
$CeZrO_{4-\delta}$	50	93	4.3	1.4	0.5	0.8	47
$PH-CeO_2/ZrO_2$	44	79	2.1	4.5	8.0	6.4	35

[a]Reaction conditions: Temperature 550°C, LHSV 3h^{-1} with respect to EB, GHSV 2400 h^{-1} with respect to Oxygen, 1 atmosphere pressure, 1mL catalyst. [d]ST-Styrene, [e]BZ-Benzene, [f]TU-Toluene, [g]SO-Styrene oxide.

INFLUENCE OF OXIDANTS:

To study the influence of participation of oxidants, the reaction was carried with and without oxidants at optimized reaction condition which will reveal the participation of lattice oxygen or oxidant in the reaction. The reaction without oxidant at optimized conditions was carried out and it shows only 23% conversion of EB and 22% yield of ST which indicates, that the lattice oxygen drives the reaction. To confirm the result, we introduced oxygen as an oxidant into the reaction; the conversion and yield increased to 52% and 48% (Fig.12.). It may be due to facile dissociation of molecular oxygen on the surface of the catalyst, which is further reactive towards EB to convert styrene. The removal of lattice oxygen is replenished by substituting gaseous molecular oxygen into the lattice which enhances the catalytic activity.[38]

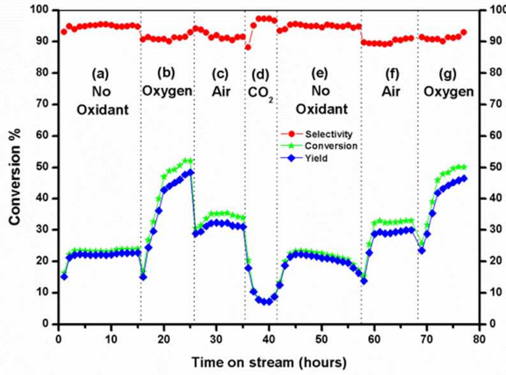

Fig.12. Different oxidant study of oxidative dehydrogenation of EB to ST over $CeZrO_{4-\delta}$ catalyst (Reaction Conditions: 550˚C, LHSV 3 h^{-1} with respect to EB and 1 atmosphere pressure, 1mL catalyst). (a) Without Oxidant, (b) With Oxygen (GHSV 2400 h^{-1}), (c) With Air (GHSV 10800 h^{-1}), (d) With Carbon dioxide (GHSV 2400 h^{-1}), (e) Without Oxidant, (f) With Air (GHSV 10800 h^{-1}), (g) With Oxygen (GHSV 2400 h^{-1})

ODH of EB was studied with soft oxidants like CO_2 and air continuously in the stream. EB conversion and ST yield for CO_2 as an oxidant were low compared to other oxidants; it may be due to coke formation or inability to activate the CO_2. There is not much replenishing of lattice oxygen by air, so air as an oxidant shows less conversion than Oxygen. If oxygen is used as an oxidant, replenishing of the lattice oxygen by molecular oxygen leads to enhancement in the catalytic activity and in turn it shows maximum conversion and selectivity. Maximum EB conversion was obtained for oxygen as an oxidant. **Table.3.** shows the effect of various oxidants on catalytic activity of $CeZrO_{4-\delta}$ for ODH of EB.

Table.3. Effect of various oxidants on catalytic activity of $CeZrO_{4-\delta}$ for ODH of EB

Oxidant	Conversion % (EB)	Selectivity %					Yield % (ST)
		ST[d]	BZ[e]	TU[f]	SO[g]	CO_x	
Nil	23	94	4.0	2.0	--	--	22
Oxygen[a]	51	92	4.8	1.0	0.4	0.8	47
Air[b]	33	91	2.0	1.0	5.0	1.0	31
Carbon dioxide[c]	07	97	2.0	0.6	--	0.4	7

[a]GHSV 2400 h^{-1} with respect to Oxygen, [b]GHSV 10800 h^{-1} with respect to air, [c]GHSV 2400 h^{-1} with respect to Carbon dioxide. (Reaction conditions: Temperature 550°C, LHSV 3 h^{-1} with respect to EB, 1 atmosphere pressure, 1mL catalyst). [d]ST-Styrene, [e]BZ-Benzene, [f]TU-Toluene, [g]SO-Styrene oxide.

Stable conversion and yield were obtained without oxidant upto 15 hours. After that oxygen was introduced as an oxidant, the conversion and yield attained maximum. Without oxidant, the conversion was only 23% which might be possibly due to minimum availability of lattice oxygen. If oxygen is introduced into reaction, conversion suddenly increases to 40% this may be ease of availability and replenishment of lattice oxygen. This catalyst shows stable conversion and yield with different oxidants up to 72 hours.

CONCLUSION:

CeO_2, ZrO_2, $CeZrO_{4-\delta}$ and $PH-CeO_2/ZrO_2$ catalyst were successfully synthesized by gel-combustion and physical mixture method. Catalytic activity was performed using fixed bed continuous up flow reactor (FBR) and the catalysts were characterized by XRD, HRTEM, Raman spectroscopy, APPES, TGA and N_2 adsorption. Fluorite $CeZrO_{4-\delta}$ catalyst shows maximum conversion of 50% towards EB and selectivity of 93% towards styrene. Other catalysts (CeO_2, ZrO_2 and PH-CeO_2/ZrO_2) show less catalytic activity compared to fluorite $CeZrO_{4-\delta}$ catalyst. Fluorite structure of $CeZrO_{4-\delta}$ catalyst was confirmed by XRD. Presence of Ce +3 and Ce+4 oxidation state and oxygen vacancies of the catalyst favours the ODH reaction, which was supported by the XPS spectra. Fluorite $CeZrO_{4-\delta}$ catalyst was thermally stable up to 72 hours time on stream at optimized reaction conditions, which shows approximately 1-2% decrease in conversion and selectivity, which is just marginal. The morphology and the structure of the fluorite $CeZrO_{4-\delta}$ catalyst were unchanged after 72 hours reaction which was confirmed by HRTEM and XRD. The fluorite $CeZrO_{4-\delta}$ catalyst shows better catalytic activity among the catalysts studied for this particular reaction.

Acknowledgements

TR and KP thanks to SERB-DST for funding (SR/S1/PC-17/2011)

Notes and references

[a]Catalysis Division, CSIR-National Chemical Laboratory, Dr.Homi Bhabha Road, Pune - 411 008, India.
[b]Chemistry Division, Bhabha Atomic Research Centre, Mumbai- 400 085, India
[*]Corresponding Author; Phone No +91-020-25902006, t.raja@ncl.res.in
Phone No +91-022-25595330, aktyagi@barc.gov.in

See DOI: 10.1039/b000000x/

1. R. R. Miller, R. Newhook and A. Poole, *Critical Reviews in Toxicology*, 1994, **24**, S1-S10.
2. E. H. Lee, *Catalysis Reviews*, 1974, **8**, 285-305.
3. M.-o. Sugino, H. Shimada, T. Turuda, H. Miura, N. Ikenaga and T. Suzuki, *Applied Catalysis A: General*, 1995, **121**, 125-137.
4. Y. Sakurai, T. Suzaki, K. Nakagawa, N.-o. Ikenaga, H. Aota and T. Suzuki, *Journal of Catalysis*, 2002, **209**, 16-24.
5. N. R. Shiju, M. Anilkumar, S. P. Mirajkar, C. S. Gopinath, B. S. Rao and C. V. Satyanarayana, *Journal of Catalysis*, 2005, **230**, 484-492.
6. P. Kuśtrowski, L. Chmielarz, R. Dziembaj, P. Cool and E. F. Vansant, *The Journal of Physical Chemistry A*, 2004, **109**, 330-336.
7. A. K. Venugopal, A. T. Venugopalan, P. Kaliyappan and T. Raja, *Green Chemistry*, 2013, **15**, 3259-3267.
8. B. M. Reddy, P. Lakshmanan, S. Loridant, Y. Yamada, T. Kobayashi, C. López-Cartes, T. C. Rojas and A. Fernández, *The Journal of Physical Chemistry B*, 2006, **110**, 9140-9147.
9. K. Sivaranjani, A. Verma and C. S. Gopinath, *Green Chemistry*, 2012, **14**, 461-471.
10. B. M. Reddy, K. N. Rao, G. K. Reddy, A. Khan and S.-E. Park, *The Journal of Physical Chemistry C*, 2007, **111**, 18751-18758.
11. L. Wang , J. J. Delgado , B. Frank , Z. Zhang, Z. Shan, D. S. Su and F.-S. Xiao, *ChemSusChem*, 2012, **5**, 687-693.
12. Y. Ohishi, T. Kawabata, T. Shishido, K. Takaki, Q. Zhang, Y. Wang, K. Nomura and K. Takehira, *Applied Catalysis A: General*, 2005, **288**, 220-231.
13. A. Trovarelli, *Catalysis Reviews*, 1996, **38**, 439-520.
14. J. Kašpar, P. Fornasiero and M. Graziani, *Catalysis Today*, 1999, **50**, 285-298.
15. H. C. Yao and Y. F. Y. Yao, *Journal of Catalysis*, 1984, **86**, 254-265.
16. J. Xu, L.-C. Wang, Y.-M. Liu, Y. Cao, H.-Y. He and K.-N. Fan, *Catal Lett*, 2009, **133**, 307-313.
17. M. Shen, J. Wang, J. Shang, Y. An, J. Wang and W. Wang, *The Journal of Physical Chemistry C*, 2009, **113**, 1543-1551.
18. L. Vivier and D. Duprez, *ChemSusChem*, 2010, **3**, 654-678.
19. J. Beckers and G. Rothenberg, *Green Chemistry*, 2010, **12**, 939-948.
20. E. Aneggi, C. de Leitenburg, G. Dolcetti and A. Trovarelli, *Catalysis Today*, 2006, **114**, 40-47.
21. M. Pijolat, M. Prin, M. Soustelle, O. Touret and P. Nortier, *Journal of the Chemical Society, Faraday Transactions*, 1995, **91**, 3941-3948.
22. R. Di Monte and J. Kašpar, *Catalysis Today*, 2005, **100**, 27-35.
23. S. N. Achary, S. K. Sali, N. K. Kulkarni, P. S. R. Krishna, A. B. Shinde and A. K. Tyagi, *Chemistry of Materials*, 2009, **21**, 5848-5859.
24. I. Atribak, A. Bueno-Lopez, A. Garcia-Garcia and B. Azambre, *Physical Chemistry Chemical Physics*, 2010, **12**, 13770-13779.
25. D. G. Lamas, G. E. Lascalea, R. E. Juarez, E. Djurado, L. Perez and N. E. Walsoe de Reca, *Journal of Materials Chemistry*, 2003, **13**, 904-910.
26. H. Vidal, J. Kašpar, M. Pijolat, G. Colon, S. Bernal, A. Cordón, V. Perrichon and F. Fally, *Applied Catalysis B: Environmental*, 2000, **27**, 49-63.
27. B. Reddy, P. Bharali, G. Thrimurthulu, P. Saikia, L. Katta and S.-E. Park, *Catal Lett*, 2008, **123**, 327-333.
28. B. Reddy and A. Khan, *Catal Surv Asia*, 2005, **9**, 155-171.
29. D. Zhao, J. Sun, Q. Li and G. D. Stucky, *Chemistry of Materials*, 2000, **12**, 275-279.
30. A. Pfau and K. D. Schierbaum, *Surface Science*, 1994, **321**, 71-80.
31. L. Jiang, H. Zhu, R. Razzaq, M. Zhu, C. Li and Z. Li, *International Journal of Hydrogen Energy*, 2012, **37**, 15914-15924.
32. F. Zhang, P. Wang, J. Koberstein, S. Khalid and S.-W. Chan, *Surface Science*, 2004, **563**, 74-82.
33. A. Bensalem, F. Bozon-Verduraz, M. Delamar and G. Bugli, *Applied Catalysis A: General*, 1995, **121**, 81-93.
34. A. Galtayries, R. Sporken, J. Riga, G. Blanchard and R. Caudano, *Journal of Electron Spectroscopy and Related Phenomena*, 1998, **88–91**, 951-956.
35. A. E. Nelson and K. H. Schulz, *Applied Surface Science*, 2003, **210**, 206-221.
36. H. Xu, D.-H. Qin, Z. Yang and H.-L. Li, *Materials Chemistry and Physics*, 2003, **80**, 524-528.
37. K. N. Rao, B. M. Reddy, B. Abhishek, Y.-H. Seo, N. Jiang and S.-E. Park, *Applied Catalysis B: Environmental*, 2009, **91**, 649-656.
38. T. M. Sankaranarayanan, R. H. Ingle, T. B. Gaikwad, S. K. Lokhande, T. Raja, R. N. Devi, V. Ramaswamy and P. Manikandan, *Catal Lett*, 2008, **121**, 39-51.